P2P Ranging-Based Cooperative Localization Method for a Cluster of Mobile Nodes Containing IR-UWB PHY

Seong Yun Cho, Joo Young Kim, and Munkhzul Enkhtur

The problem of pedestrian localization using mobile nodes containing impulse radio ultra wideband (IR-UWB) is considered. IEEE 802.15.4a-based IR-UWB can achieve accurate ranging. However, the coverage is as short as 30 m, owing to the restricted transmit power. This factor may cause a poor geometric relationship among the mobile nodes and anchor nodes in certain environments. To localize a group of pedestrians accurately, an enhanced cooperative localization method is proposed. We describe a sequential algorithm and define problems that may occur in the implementation of the algorithm. To solve these problems, a batch algorithm is proposed. The batch algorithm can be carried out after performing the sequential algorithm to linearize the nonlinear range equation. When a sequential algorithm cannot be performed due to a poor geometric relationship among nodes, a batch algorithm can be carried out directly. Herein, Monte Carlo simulations are presented to illustrate the proposed method and verify its performance.

Keywords: Cooperative localization, P2P ranging, IR-UWB, least squares.

Manuscript received Dec. 4, 2012; revised May 13, 2013; accepted June 3, 2013.

Seong Yun Cho (phone: +82 53 600 5584, sycho@kiu.kr) was with the IT Convergence Technology Research Laboratory, ETRI, Daejeon, Rep. of Korea, and is now with the Department of Applied Robotics, Kyungil University, Gyeongsan, Rep. of Korea.

Joo Young Kim (kimjy@etri.re.kr) is with the IT Convergence Technology Research Laboratory, ETRI, Daejeon, Rep. of Korea.

Munkhzul Enkhtur (mr_enkhtor@etri.re.kr) is with the IT Convergence Technology Research Laboratory, ETRI, Daejeon, Rep. of Korea, and also with the Department of Mobile Communication & Digital Broadcasting Engineering, University of Science & Technology, Daejeon, Rep. of Korea.

I. Introduction

Location information has been one of the important items in the emerging location-based service (LBS) industry [1]. In particular, pedestrian navigation services have become hot LBS applications for smartphones. To provide location information, the Global Positioning System (GPS) is generally used. However, a GPS signal cannot be used continuously in an urban indoor area because of signal blockage. To overcome these restrictions, several alternative localization methods have been investigated using a mobile communication infrastructure [2]-[4], wireless communication infrastructure [5]-[12], a wireless sensor network (WSN) [13]-[20], and so on. We can use mobile communication signals, such as CDMA and WiBro, for making calls without a shadow area. Moreover, we can use a Wi-Fi signal indoors and in public places for Internet access. If we can use these types of signals in a GPS signal-blocked area, location information can be obtained based on a wireless localization method.

The performance of a wireless localization method depends on the signal characteristics of the physical layer (PHY) used for ranging, the geometric relationship among the infrastructure and mobile nodes (MNs), the localization algorithm, and so on. The most well-known PHY containing sufficient signal characteristics for ranging is impulse radio ultra wideband (IR-UWB) based on IEEE 802.15.4a, which has an absolute bandwidth of at least 500 MHz or a fractional bandwidth of larger than 20%. Owing to the inverse relationship between the bandwidth and duration of a signal, an IR-UWB signal has very short waveforms, usually on the order of a nanosecond.

There are many advantages to a short duration pulse, such as an extremely fine time resolution, multipath robustness, high ranging accuracy, an enhanced capability to penetrate walls, and a low probability of detection. A high ranging accuracy is caused by a fine time resolution [21]. The best achievable accuracy of a distance estimate derived from the time of arrival (ToA) estimation satisfies the following inequality [22].

$$\sqrt{Var(\hat{d})} \geq \frac{c}{2\sqrt{2}\pi\sqrt{SNR}\beta} \quad , \tag{1}$$

where $\hat{d}$ is the distance estimate, c is the speed of light, SNR is the signal-to-noise ratio, and β is the bandwidth.

As IR-UWB signals occupy a very large portion of the spectrum, a set of regulations have been imposed on the transmitter of IR-UWB signals by the Federal Communications Commission (FCC) to prevent significant interference with other wireless communication systems in the same frequency spectrum. According to the FCC regulations, the average power spectral density must not exceed –41.3 dBm/MHz over the frequency band of 3.1 GHz to 10.6 GHz [23]. Owing to this regulation, the propagation range/ranging coverage is unavoidably as short as 30 m when the data rate is 850 kbps. This may cause a poor geometric relationship among the infrastructure and MNs and poor localization results. To enhance the localization accuracy and availability, a new paradigm has emerged, namely cooperative localization [24], [25]. This topic has been widely studied in the area of wireless sensor networks for estimating the location of arbitrarily deployed sensors [13]-[20]. Several localization algorithms have also been investigated with a focus on the geometric dilution of precision and the Cramér-Rao lower bound of the estimation methods, among others.

In this paper, the targets to be localized are not considered as sensors in a WSN but MNs, such as smartphones owned by pedestrians with the same objective. It is assumed that IR-UWB is installed on a smartphone and the application areas are special environments, such as a soccer field, amusement park, or scene of a fire or battle. In these environments, only a small number of anchor nodes (ANs) may be installed, owing to a technical restriction, destruction, cost, and so on. Each user possesses an MN. However, there may not be an adequate number of ANs for wireless localization in a wide field. In this case, a localization method based on peer-to-peer (P2P) communication can be used [24]. P2P communication means a set of MN connections for sharing information rather than a connection by a server. First, a cooperative localization method using a sequential algorithm (CLM-SA) is described [24]. The location of the MNs is estimated sequentially using an adaptive direct solution method. This method may have several problems owing to the poor geometry relationship of the MNs and insufficient measurements. In this paper, a cooperative localization method using a batch algorithm (CLM-BA) is proposed to enhance the performance of the sequential algorithm. This method has certain merits; for example, the estimation accuracy is enhanced slightly owing to an improvement of the geometric relationship among nodes, and the method can be used when some links among ANs and MNs are disconnected from movement of the MNs. To verify the performance of the proposed method, Monte Carlo simulations are carried out.

The rest of the paper is arranged as follows. In section II, the CLM-SA is described and some problems that may occur in the CLM-SA are defined. The CLM-BA, which is used to solve these problems, is described in section III. In section IV, a performance evaluation of the proposed method is carried out. Finally, some concluding remarks are provided in the last section.

II. Conventional CLM and Problem Statement

1. Need for Cooperative Localization

In ranging-based wireless localization, several estimation methods have been used, such as an approximated linear estimator (ALE) based on least squares (LS) or the maximum likelihood method and the nonlinear direct solution method (NDSM) [24], [26]-[28]. There must be more than three reference nodes (RNs) connected to the MN to be localized, as can be seen in Fig. 1(a). In this figure, the location of MN_1 can be estimated using the connection information with RN_1, RN_2, and RN_5. The connection information includes the location data of the RNs and the distance estimates between the MN and each RN to formulate the following equation:

$$\rho_{(i)-j} = \sqrt{(x_{MN_j} - x_{RN_i})^2 + (y_{MN_j} - y_{RN_i})^2}, \tag{2}$$

where x and y are coordinate axes and where i and j are the IDs for the RN and MN, respectively. Using this equation, the locations of the MNs can be estimated based on the ALE or NDSM.

The RN_5 is removed for case II shown in Fig. 1(b). If the MNs are not connected to each other, only NDSM can be used to estimate the locations of the MNs. However, it is difficult to select an exact solution between a true solution (TS) and false solution (FS), as denoted in Fig. 1(b). If the connection information between the MNs can be obtained, it becomes easy to estimate the exact locations of the MNs based on the concept of the CLM.

2. CLM-SA

In the WSN area, several methods for estimating the

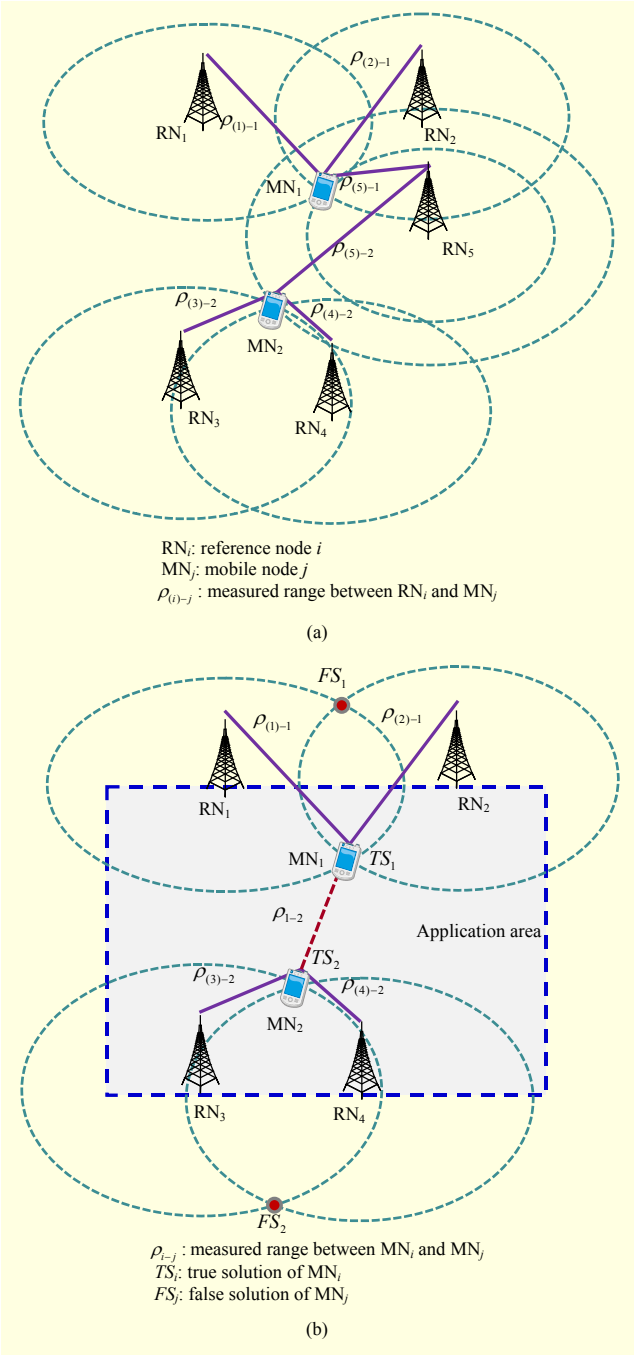

Fig. 1. Necessity of cooperative localization: (a) case I and (b) case II.

locations of freely deployed sensor nodes have been investigated [13]-[20]. One of the main methods is the CLM-SA. The locations of the MNs are estimated sequentially from the MN connected to the RNs. First, the number of reference nodes (NRN) for each MN is calculated. The reference node denotes the AN or pre-localized MN connected to the MN to be estimated at this step. The MN that has the largest NRN among the MNs is then selected. If the largest NRN is greater than or equal to 3, ALE or NDSM can be used to estimate the location of the selected MN. If the largest NRN is equal to 2, only NDSM can be used. In this case, a solution selection problem between two candidate solutions must be solved [24]. If the largest NRN is equal to 1, the Cell-ID method is used in conventional methods. If the largest NRN is 0 or all MNs are localized, the CLM-SA is closed. Consequently, the MN whose NRN is larger than or equal to 2 can be localized based on the NDSM.

Two candidate solutions of MN_j are calculated using the NDSM as follows [24], [26]:

$$\begin{bmatrix} \hat{x}_{MN_j}(i) \\ \hat{y}_{MN_j}(i) \end{bmatrix} = (H^T H)^{-1} H^T \left\{ R_a + \frac{1 - 2R_a^T L R_b}{2R_b^T L R_b} + (-1)^i \frac{\sqrt{(2R_a^T L R_b - 1)^2 - 4R_a^T L R_b R_a^T L R_a}}{2R_b^T L R_b} R_b \right\}, \quad (3)$$

where $i \in \{1, 2\}$,

$$H = \begin{bmatrix} -2x_{RN_{S(1)}} & -2y_{RN_{S(1)}} \\ \vdots & \vdots \\ -2x_{RN_{S(n)}} & -2y_{RN_{S(n)}} \end{bmatrix}, \quad (4\text{-}1)$$

$$R_a = \begin{bmatrix} \rho_{S(1)-j}^2 - (x_{RN_{S(1)}}^2 + y_{RN_{S(1)}}^2) \\ \vdots \\ \rho_{S(n)-j}^2 - (x_{RN_{S(n)}}^2 + y_{RN_{S(n)}}^2) \end{bmatrix}, \quad (4\text{-}2)$$

$$R_b = [\overbrace{-1 \quad \cdots \quad -1}^{n}]^T, \quad (4\text{-}3)$$

$$L = H\left[(H^T H)^{-1}\right]^2 H^T, \quad (4\text{-}4)$$

where n is the NRN, $[x_{RN_{S(i)}} \quad y_{RN_{S(i)}}]^T$ is the location data of the reference node whose ID is $S(i)$, and $\rho_{S(i)-j}$ is the distance estimate between the MN_j and $RN_{S(i)}$.

One correct solution between two candidate solutions must be selected. Usually, the one solution whose residual is smaller than the other is selected [24], [26]. The residuals are calculated as follows:

$$e(k) = \sum_{i=1}^{n} \left| \rho_{S(i)-j} - \sqrt{(x_{RN_{S(i)}} - \hat{x}_{MN_j}(k))^2 + (y_{RN_{S(i)}} - \hat{y}_{MN_j}(k))^2} \right|, \quad (5)$$

where $n \geq 3$ and $k \in \{1, 2\}$.

In the case of Fig. 1(b), the NRN connected to each MN is 2. In this case, it is difficult to select the correct solution based on the residual test. Fortunately, useful information exists: the application area and distance measurement between two MNs. Using this information, the location of the two MNs can be estimated accurately as follows:

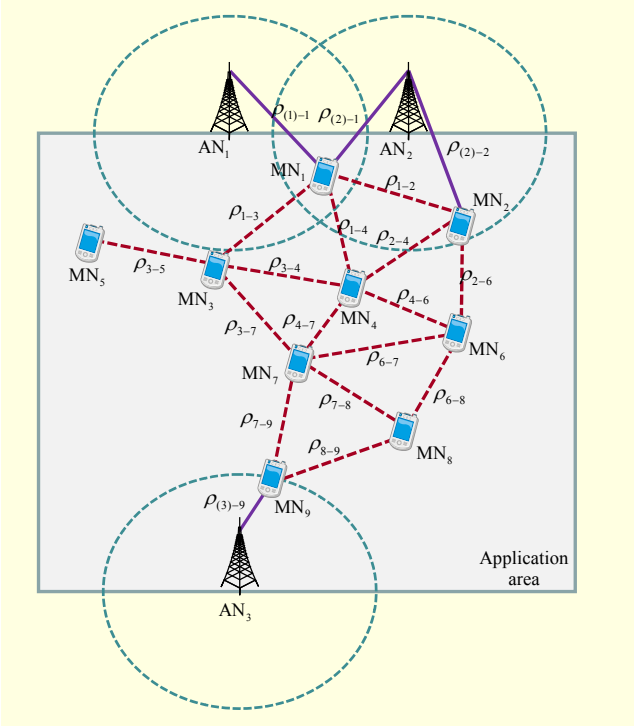

Fig. 2. Example environment.

$$\left(\hat{P}_{MN_1}(\bar{i})\ \hat{P}_{MN_2}(\bar{j})\right) = \arg\min_{i,j\in\{1,2\}} \left|\rho_{1-2} - \sqrt{(\hat{x}_{MN_1}(i)-\hat{x}_{MN_2}(j))^2+(\hat{y}_{MN_1}(i)-\hat{y}_{MN_2}(j))^2}\right|, \tag{6}$$

where $\hat{P}_{MN_k}(\bar{i})$ is the i-th candidate solution of the MN_k.

Additional information is the application area. That is, the candidate solution that locates out of the application area denoted in Fig. 1(b) is the FS.

3. Problem Statement

When a cooperative localization method is applied to MNs possessed by pedestrians for the same objective, such as a battle, firefighting, or a sporting event, it becomes slightly different from that for WSN applications. The primary difference is the mobility of the nodes. In this case, some problems may occur when the CLM-SA is used as the main algorithm. In this paper, we define the following assumption and problems that must be solved.

Assumption. Figure 2 shows an example of a localizing of the MNs used in this application. In the application area, there are only three ANs. In the figure, a circle indicates the coverage of an AN. It can be seen that three ANs cannot cover the entire application area. Fortunately, the MNs are connected to each other. The range information between the connected MNs is then updated periodically.

Problem 1. When the number of ANs connected to an MN is smaller than two owing to the movement of the MNs under the assumed environment, the MNs cannot be localized based on the CLM-SA. If some MNs move, the MNs can be localized by using the information of the unmoved MNs within the coverage. When all the MNs move, however, the CLM-SA cannot provide the updated location information.

Problem 2. The information on the MNs and ANs that have a multihop connection with the MN to be localized in this step cannot be used. For example, the information of AN_3 in Fig. 2 cannot be used to localize MN_1.

Problem 3. A singular problem may occur owing to the poor geometry of the reference nodes.

III. CLM-BA

1. CLM-BA

In this work, we consider a CLM using the batch algorithm to overcome the problems mentioned above. The basic concept of this method is the ALE. The following distance equation is linearized based on the first-order Taylor series expansion.

$$\begin{aligned}\rho_{i-j} &= \sqrt{(x_{MN_i}-x_{MN_j})^2+(y_{MN_i}-y_{MN_j})^2} \\ &\cong \bar{\rho}_{i-j} + \bar{l}^x_{i-j}\delta x_i - \bar{l}^x_{i-j}\delta x_j + \bar{l}^y_{i-j}\delta y_i - \bar{l}^y_{i-j}\delta y_j,\end{aligned} \tag{7}$$

where

$$\bar{\rho}_{i-j} = \sqrt{(\bar{x}_i-\bar{x}_j)^2+(\bar{y}_i-\bar{y}_j)^2}, \tag{8-1}$$

$$\bar{l}^x_{i-j} = \frac{\bar{x}_i-\bar{x}_j}{\bar{\rho}_{i-j}}, \tag{8-2}$$

$$\bar{l}^y_{i-j} = \frac{\bar{y}_i-\bar{y}_j}{\bar{\rho}_{i-j}}, \tag{8-3}$$

where $\bar{P}_{MN_i} \equiv (\bar{x}_i, \bar{y}_i)$ denotes the nominal point of $P_{MN_i} \equiv (x_i, y_i)$ for a linearization of a nonlinear equation, and $\delta P_{MN_i} \equiv (\delta x_i, \delta y_i)$ indicates the difference between the nominal point and the true location.

Equation (7) can be rearranged into the following matrix form.

$$\begin{aligned}\delta\rho_{i-j} &\equiv \rho_{i-j} - \bar{\rho}_{i-j} \\ &= \bar{l}^x_{i-j}\delta x_i - \bar{l}^x_{i-j}\delta x_j + \bar{l}^y_{i-j}\delta y_i - \bar{l}^y_{i-j}\delta y_j \\ &= \begin{bmatrix}\bar{l}^x_{i-j} & \bar{l}^y_{i-j} & -\bar{l}^x_{i-j} & -\bar{l}^y_{i-j}\end{bmatrix}\begin{bmatrix}\delta x_i \\ \delta y_i \\ \delta x_j \\ \delta y_j\end{bmatrix}.\end{aligned} \tag{9}$$

When AN_i and MN_i are connected, (9) can be changed as follows:

$$\delta\rho_{(i)-j} = \begin{bmatrix} 0 & 0 & -\bar{l}^{x}_{(i)-j} & -\bar{l}^{y}_{(i)-j} \end{bmatrix} \begin{bmatrix} \delta x_{(i)} \\ \delta y_{(i)} \\ \delta x_j \\ \delta y_j \end{bmatrix}. \quad (10)$$

If the number of MNs is n and the number of connections is m, the main equation for the CLM-BA is formulated as follows.

$$\begin{aligned} Y &= M\delta Z \\ &\leftrightarrow \begin{bmatrix} \delta\rho_{i_1-j_1} & \delta\rho_{i_2-j_2} & \cdots & \delta\rho_{i_n-j_n} \end{bmatrix}^T \\ &= M\begin{bmatrix} \delta x_1 & \delta y_1 \vdots \delta x_2 & \delta y_2 \vdots \cdots \vdots \delta x_n & \delta y_n \end{bmatrix}^T, \end{aligned} \quad (11)$$

where M is formulated according to the connection information between the MNs and ANs based on (9) and (10).

An MN in which NRN is equal to 1 must be excluded in the processing of the CLM-BA owing to the observability problem. δZ in (11) can be estimated using the LS method as

$$\delta\hat{Z} = \left(M^T M\right)^{-1} M^T Y \ . \quad (12)$$

The estimated error terms are added to the nominal points to estimate the locations of the MNs.

$$\begin{bmatrix} \hat{P}_{MN_1} \\ \vdots \\ \hat{P}_{MN_n} \end{bmatrix} = \begin{bmatrix} \overline{P}_{MN_1} \\ \vdots \\ \overline{P}_{MN_n} \end{bmatrix} + \delta\hat{Z} \quad (13)$$

The estimated locations are set as new nominal points for repeating the same procedure. If (12) converges to near zero, the locations of the MNs are finally decided using (13).

In this method, an important factor that cannot be neglected is the initial nominal points of the MNs for linearizing nonlinear (7). If the initial errors of the nominal points are large, (12) may diverge or the finally determined locations of the MNs may have large errors. To solve this problem, in this paper, the initial nominal points are set as the results of the CLM-SA.

Figure 3 shows the flow chart of the CLM proposed in this paper. Initially, the connection numbers between MNs and ANs are calculated. If there is an MN connected to at least two ANs, the CLM-SA is performed. The solution of the CLM-SA is used to set the nominal points for the CLM-BA. The CLM-BA is then carried out. If there is not an MN connected to multiple ANs after the MNs move, the CLM-BA is used directly. In this case, the nominal points for the CLM-BA are set as the last solution of the CLM-SA.

Problems 1 and 2 can be solved using the proposed CLM-BA. The other problems must be overcome to achieve the successful CLM-BA. In the next subsection, a tip for solving Problem 3 is provided.

2. Tip for Solving Problem 3

To solve Problem 3, the cause of the singular problem is analyzed. Irrespective of the relation between the MN and RNs, the inverse calculation may fail in (3) and (4-4) owing to the geometry of the RNs. First, the determinant of $H^T H$ is calculated as

$$\begin{aligned} \delta &= \det(H^T H) \\ &= \left(\sum_{i=1}^{n} x^2_{RN_{S(i)}}\right)\left(\sum_{i=1}^{n} y^2_{RN_{S(i)}}\right) - \left(\sum_{i=1}^{n} x_{RN_{S(i)}} y_{RN_{S(i)}}\right)^2, \end{aligned} \quad (14)$$

where n is the NRN. If δ in (14) is equal to 0, the singular problem occurs. For computational simplicity, it is assumed that the NRN is equal to 2. The singular problem occurs in the following case.

$$y_{RN_{S(2)}} = \frac{y_{RN_{S(1)}}}{x_{RN_{S(1)}}} x_{RN_{S(2)}} \ . \quad (15)$$

Therefore, when the line connecting the two reference nodes passes through the origin, the singular problem occurs. To avoid this problem, an efficient method is presented, as shown in Fig. 4. If δ is equal to 0, $RN_{S(1)}$ is set as a pivot. Then, $RN_{S(2)}$ is rotated on the pivot by θ, as follows:

$$RN'_{S(2)} = M_R\left(RN_{s(2)} - RN_{s(1)}\right) + RN_{s(1)} \ , \quad (16)$$

where

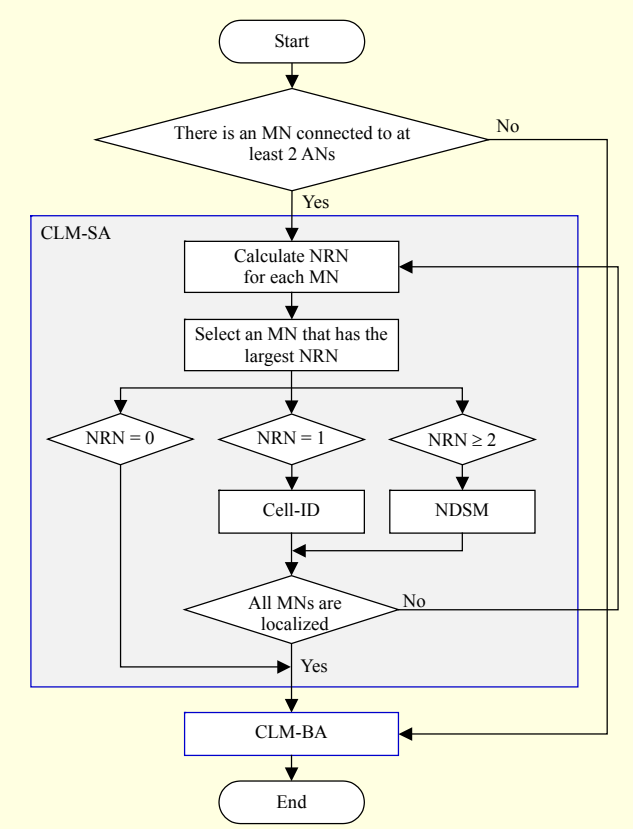

Fig. 3. Flow chart of cooperative localization method.

ETRI Journal, Volume 35, Number 6, December 2013
http://dx.doi.org/10.4218/etrij.13.0112.0823

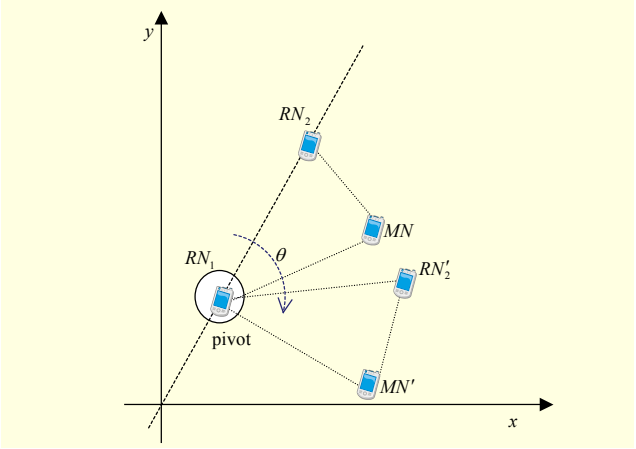

Fig. 4. Method for avoiding singular problem.

$$M_R = \begin{bmatrix} \cos\theta & \sin\theta \\ -\sin\theta & \cos\theta \end{bmatrix}. \quad (17)$$

$RN'_{S(2)}$ instead of $RN_{S(2)}$ is inserted into (4-1) and (4-2). Then, L in (4-4) can be calculated without a singular problem. However, the estimated location of the MN is MN', as shown in Fig. 4. Therefore, the final solution can be amended as follows:

$$M\hat{N} = M_R^{-1}\left(MN' - RN_{s(1)}\right) + RN_{s(1)} \quad (18)$$

IV. Simulation Results and Analysis

To verify the performance of the presented algorithm, some Monte Carlo simulations are performed, as shown in Fig. 5. First, the CLM-SA is performed on the given simulation environment. The solution of the CLM-SA is used for the nominal point of the CLM-BA. After carrying out the CLM-BA, the performances of the CLM-SA and CLM-BA are compared. The simulation environment is set as shown in Fig. 2. There are nine MNs and three ANs. The MN/AN coverage is set to 40 m. It is assumed that each MN is connected with the MNs and ANs within the coverage area, as can be seen in Fig. 2. The ranging between the connected nodes is conducted preferentially. The statistical error of the estimated range is set as white Gaussian noise with 30 cm for simulation 1 and 60 cm for simulation 2. For the Monte Carlo simulation, 1,000 ensembles of ranging errors are generated.

First, the CLM-SA is processed in the following sequence.

- Step 1: MN_1 is localized using the RNs (AN_1 and AN_2).
- Step 2: MN_2 is localized using the RNs (AN_2 and MN_1).
- Step 3: MN_4 is localized using the RNs (MN_1 and MN_2).
- Step 4: MN_3 is localized using the RNs (MN_1 and MN_4).
- Step 5: MN_6 is localized using the RNs (MN_2 and MN_4).
- Step 6: MN_7 is localized using the RNs (MN_3, MN_4, and MN_6).
- Step 7: MN_8 is localized using the RNs (MN_6 and MN_7).
- Step 8: MN_9 is localized using the RNs (MN_7, MN_8, and AN_3).
- Step 9: MN_5 is localized using the RNs (MN_3).

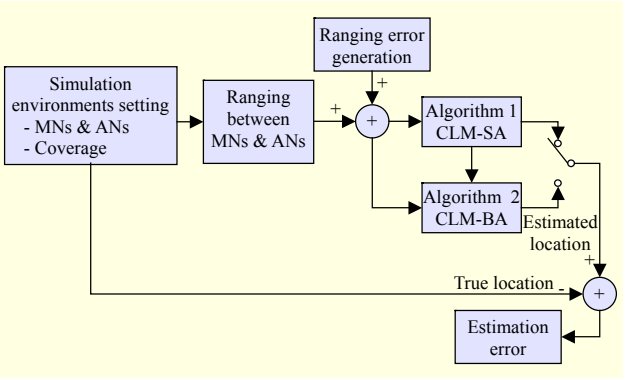

Fig. 5. Simulation configuration.

The location information of the ANs is accurate. Therefore, the MN_1 is localized using the following equation.

$$\rho_{(i)-1} + \delta\rho_{(i)-1} = \sqrt{(x_{AN_i} - x_{MN_1})^2 + (y_{AN_i} - y_{MN_1})^2}, \quad (19)$$

where $i \in \{1, 2\}$ and $\delta\rho_{(i)-1}$ is the range error included in the measurement. This range error causes a location estimation error of MN_1. In the next step, the basic equation may be distorted as follows:

$$\rho_{1-2} + \delta\rho_{1-2} = \sqrt{(x_{MN_1} + \delta\hat{x}_{MN_1} - x_{MN_2})^2 + (y_{MN_1} + \delta\hat{y}_{MN_1} - y_{MN_2})^2}. \quad (20)$$

In this step, the estimation error of MN_2 is caused by a location estimation error of MN_1 as well as the range error. Therefore, the estimation errors may have a tendency to increase with the localization order.

Second, the CLM-BA is processed. In this simulation, the main equation for the CLM-BA is formulated as follows:

$$Y = M\delta Z, \quad (21)$$

where

$$\delta Z = \left[\delta x_1 \quad \delta y_1 \quad \cdots \quad \delta x_4 \quad \delta y_4 \quad \delta x_6 \quad \delta y_6 \quad \cdots \quad \delta x_8 \quad \delta y_8\right]^T, \quad (22)$$

$$Y = \left[\delta\rho_{(1)-1} \quad \delta\rho_{(2)-1} \quad \delta\rho_{(2)-2} \quad \delta\rho_{1-2} \quad \delta\rho_{1-3} \quad \delta\rho_{1-4} \quad \delta\rho_{2-4} \quad \delta\rho_{2-6} \quad \delta\rho_{3-4} \quad \delta\rho_{3-7} \quad \delta\rho_{4-6} \quad \delta\rho_{4-7} \quad \delta\rho_{6-7} \quad \delta\rho_{6-8} \quad \delta\rho_{7-8} \quad \delta\rho_{7-9} \quad \delta\rho_{8-9} \quad \delta\rho_{(3)-9}\right]^T, \quad (23)$$

$$M = \left[m_1^T \quad \cdots \quad m_{18}^T\right]^T, \quad (24)$$

where

$$m_1 = \left[-\bar{l}^x_{(1)-1} \quad -\bar{l}^y_{(1)-1} \quad 0_{1\times 14}\right], \quad (25\text{-}1)$$

$$m_2 = \left[-\bar{l}^x_{(2)-1} \quad -\bar{l}^y_{(2)-1} \quad 0_{1\times 14}\right], \quad (25\text{-}2)$$

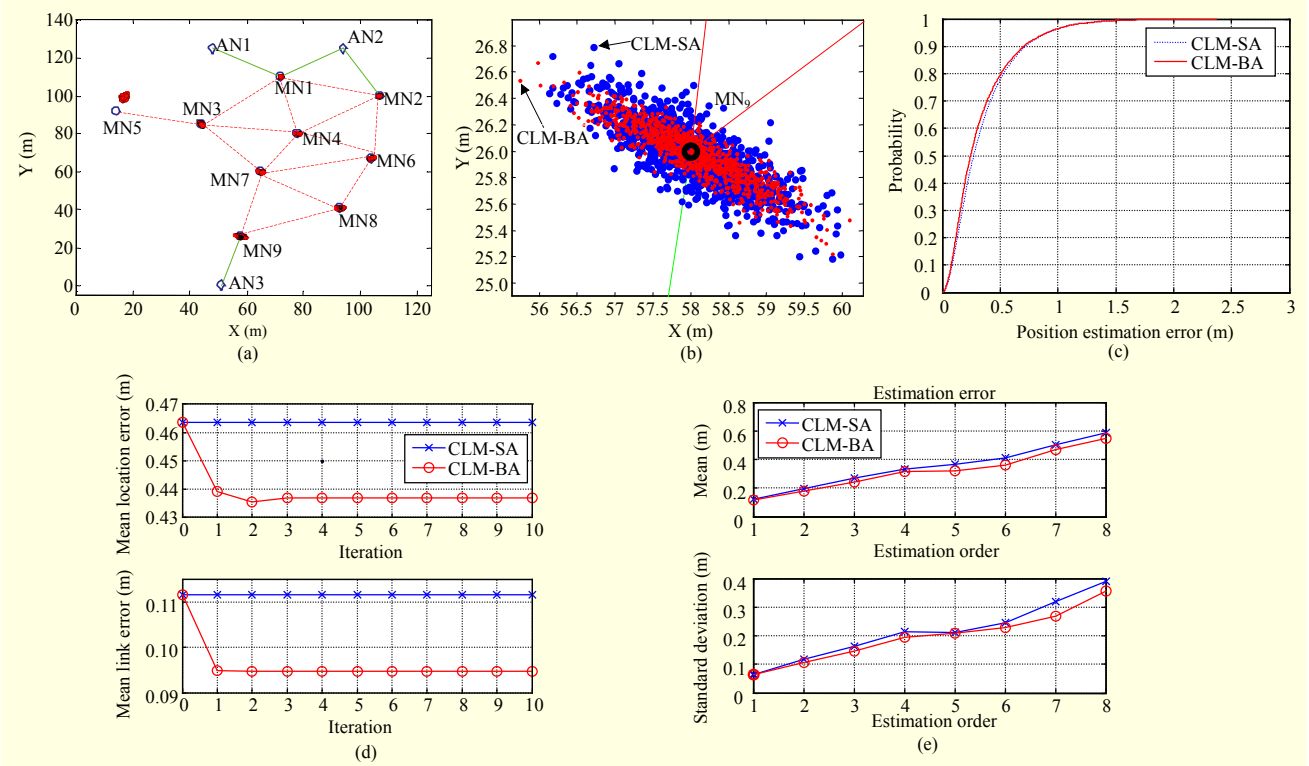

Fig. 6. Results of simulation 1 (ranging error = 30 cm, 99.7% under normal distribution): (a) estimated location of MNs, (b) estimated location of MN_9, (c) error probabilities according to algorithms (CLM-SA: 27.30 cm, CLM-BA: 24.43 cm [CEP]), (d) mean location error and mean link error, and (e) estimation error according to estimation order.

$$m_3 = \left[0_{1\times2} \quad -\bar{l}^{x}_{(2)-2} \quad -\bar{l}^{y}_{(2)-2} \quad 0_{1\times12}\right], \tag{25-3}$$

$$m_4 = \left[\bar{l}^{x}_{1-2} \quad \bar{l}^{y}_{1-2} \quad -\bar{l}^{x}_{1-2} \quad -\bar{l}^{y}_{1-2} \quad 0_{1\times12}\right], \tag{25-4}$$

$$m_5 = \left[\bar{l}^{x}_{1-3} \quad \bar{l}^{y}_{1-3} \quad 0_{1\times2} \quad -\bar{l}^{x}_{1-3} \quad -\bar{l}^{y}_{1-3} \quad 0_{1\times10}\right], \tag{25-5}$$

$$m_6 = \left[\bar{l}^{x}_{1-4} \quad \bar{l}^{y}_{1-4} \quad 0_{1\times4} \quad -\bar{l}^{x}_{1-4} \quad -\bar{l}^{y}_{1-4} \quad 0_{1\times8}\right], \tag{25-6}$$

$$m_7 = \left[0_{1\times2} \quad \bar{l}^{x}_{2-4} \quad \bar{l}^{y}_{2-4} \quad 0_{1\times2} \quad -\bar{l}^{x}_{2-4} \quad -\bar{l}^{y}_{2-4} \quad 0_{1\times8}\right], \tag{25-7}$$

$$m_8 = \left[0_{1\times2} \quad \bar{l}^{x}_{2-6} \quad \bar{l}^{y}_{2-6} \quad 0_{1\times4} \quad -\bar{l}^{x}_{2-6} \quad -\bar{l}^{y}_{2-6} \quad 0_{1\times6}\right], \tag{25-8}$$

$$m_9 = \left[0_{1\times4} \quad \bar{l}^{x}_{3-4} \quad \bar{l}^{y}_{3-4} \quad -\bar{l}^{x}_{3-4} \quad -\bar{l}^{y}_{3-4} \quad 0_{1\times8}\right], \tag{25-9}$$

$$m_{10} = \left[0_{1\times4} \quad \bar{l}^{x}_{3-7} \quad \bar{l}^{y}_{3-7} \quad 0_{1\times4} \quad -\bar{l}^{x}_{3-7} \quad -\bar{l}^{y}_{3-7} \quad 0_{1\times4}\right], \tag{25-10}$$

$$m_{11} = \left[0_{1\times6} \quad \bar{l}^{x}_{4-6} \quad \bar{l}^{y}_{4-6} \quad -\bar{l}^{x}_{4-6} \quad -\bar{l}^{y}_{4-6} \quad 0_{1\times6}\right], \tag{25-11}$$

$$m_{12} = \left[0_{1\times6} \quad \bar{l}^{x}_{4-7} \quad \bar{l}^{y}_{4-7} \quad 0_{1\times2} \quad -\bar{l}^{x}_{4-7} \quad -\bar{l}^{y}_{4-7} \quad 0_{1\times4}\right], \tag{25-12}$$

$$m_{13} = \left[0_{1\times8} \quad \bar{l}^{x}_{6-7} \quad \bar{l}^{y}_{6-7} \quad -\bar{l}^{x}_{6-7} \quad -\bar{l}^{y}_{6-7} \quad 0_{1\times4}\right], \tag{25-13}$$

$$m_{14} = \left[0_{1\times8} \quad \bar{l}^{x}_{6-8} \quad \bar{l}^{y}_{6-8} \quad 0_{1\times2} \quad -\bar{l}^{x}_{6-8} \quad -\bar{l}^{y}_{6-8} \quad 0_{1\times2}\right], \tag{25-14}$$

$$m_{15} = \left[0_{1\times10} \quad \bar{l}^{x}_{7-8} \quad \bar{l}^{y}_{7-8} \quad -\bar{l}^{x}_{7-8} \quad -\bar{l}^{y}_{7-8} \quad 0_{1\times2}\right], \tag{25-15}$$

$$m_{16} = \left[0_{1\times10} \quad \bar{l}^{x}_{7-9} \quad \bar{l}^{y}_{7-9} \quad 0_{1\times2} \quad -\bar{l}^{x}_{7-9} \quad -\bar{l}^{y}_{7-9}\right], \tag{25-16}$$

$$m_{17} = \left[0_{1\times12} \quad \bar{l}^{x}_{8-9} \quad \bar{l}^{y}_{8-9} \quad -\bar{l}^{x}_{8-9} \quad -\bar{l}^{y}_{8-9}\right], \tag{25-17}$$

$$m_{18} = \left[0_{1\times14} \quad -\bar{l}^{x}_{(3)-9} \quad -\bar{l}^{y}_{(3)-9}\right]. \tag{25-18}$$

Figure 6 shows the results of simulation 1. Figure 6(a) shows the estimated location of the MNs, Fig. 6(b) shows the enlarged estimated locations of MN_9 based on the 1,000 measurements, Fig. 6(c) shows the error probabilities according to the algorithm, and Fig. 6(d) shows the mean location error and mean link error. The mean location error and mean link error can be calculated as follows:

$$LocationError_t = \sqrt{\frac{1}{n+m}\sum_{j=1}^{m}\sum_{i=1}^{n}\left(\hat{P}_{MN_i,j,(t)} - P_{MN_i}\right)^2}, \tag{26}$$

$$LinkError_t = \sqrt{\frac{1}{n+m+\sum_{i=1}^{n} num_i}\sum_{k=1}^{m}\sum_{i=1}^{n}\sum_{j\in C(i)}\left(\hat{\rho}_{i-j,(t)} - \rho_{i-j}\right)^2}, \tag{27}$$

where m is the simulation number, n is the number of MNs, $C(i)$ is the MN ID connected to the MN_i, num_i is the number of neighbor MNs connected to the MN_i, and t is the iteration step.

http://dx.doi.org/10.4218/etrij.13.0112.0823

In addition, Fig. 6(e) shows the estimation error according to the estimation order. As shown in this figure, there seems to be a tendency to accumulate the errors from the first position estimation of MN to the last position estimation of MN, as previously mentioned.

As can be seen in Fig. 6(a), all the MNs can be localized exactly except MN_5. The location of MN_5 is estimated using the restricted area method (RAM) [29]. The estimation error of the RAM may be changed according to the geometric relation among the MNs to be estimated at this step and the other RNs. However, it can be confirmed that the estimates are near the true location. In Fig. 6(b), it can be seen that the variance of the CLM-BA solutions is slightly smaller than that of the CLM-SA solutions. This conclusion can be reconfirmed from Fig. 6(c). The statistical estimation errors for the CLM-SA and CLM-BA are 27.30 cm (CEP) and 24.43 cm (CEP), respectively. As can be seen in Fig. 6(d), the mean location error and mean link error of the CLM-BA converge into a value smaller than the CLM-SA through the iteration process. Using the CLM-BA, the mean location error and mean link error are decreased by 5.76% and 17.07%, respectively. This phenomenon is caused by the enhanced geometric relation between MNs. For example, MN_4 is localized using the relation between MN_4 and MN_1/MN_2 in the CLM-SA. On the contrary, the relation between MN_4 and five MNs (MN_1, MN_2, MN_3, MN_6, and MN_7) is used in the CLM-BA.

Figure 7 shows the results of simulation 2. We can see the same results as in simulation 1. In this case, the statistical estimation error is 53.64 cm (CEP) for the CLM-SA and 51.74 cm (CEP) for the CLM-BA.

After ten iterations in the CLM-BA, the mean location error and mean link error are decreased by 7.26% and 14.89%, respectively. The error increases with respect to the ranging error. However, the ranging data obtained using the IR-UWB is as accurate as 30 cm. Consequently, the MNs can be localized accurately based on the proposed algorithm.

Figure 8 shows the estimation results when the link between AN_1 and MN_1 is disconnected owing to the movement of the MN_1. In this case, the CLM-SA cannot be operated because there is not an MN connected with at least two ANs. There are only two ANs located in separate areas. The CLM-BA is performed using the final solution of the CLM-SA as the nominal point. As can be seen in Fig. 8, all MNs can be localized successfully. The CLM-BA can localize the MNs because the MNs and ANs share a relationship with each other, which is the attractive point of cooperative localization.

To analyze the computational complexity of the methods, the processing time is measured using the "tic/toc" command in MATLAB. The mean processing times of the CLM-SA and CLM-BA are measured as 0.001294 sec and 0.002518 sec, respectively. That is, the computational complexity of the CLM-BA is about 194.54% that of the CLM-SA.

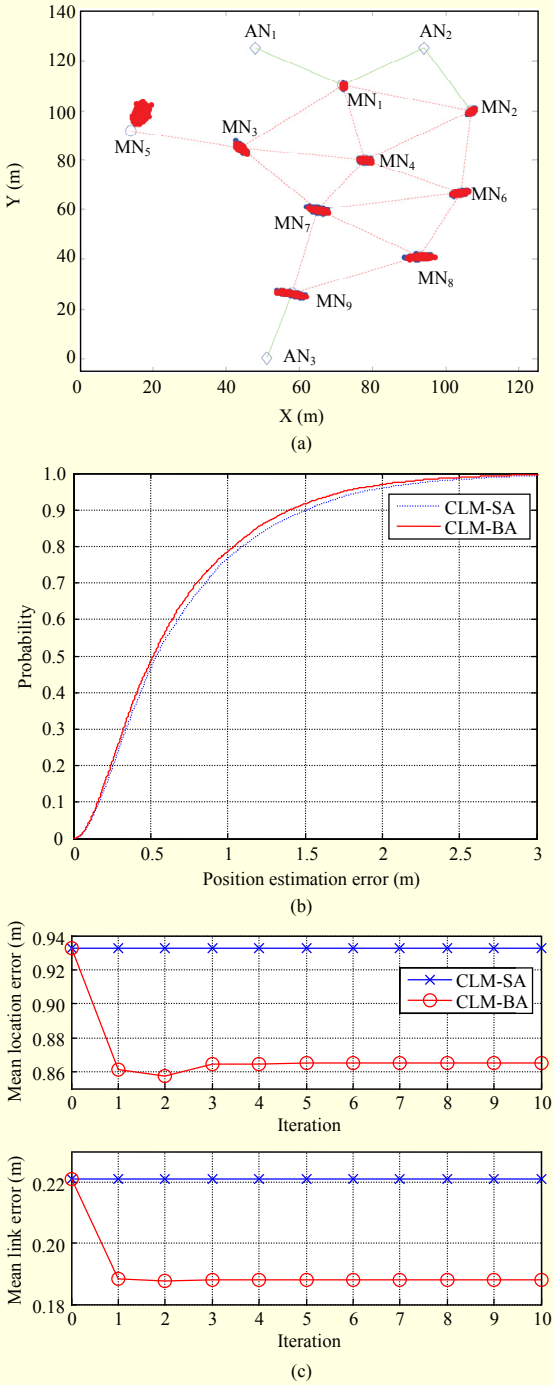

Fig. 7. Results of simulation 2 (ranging error = 60 cm, 99.7% under a normal distribution): (a) estimated location of MNs, (b) error probabilities according to algorithms (CLM-SA: 53.64 cm, CLM-BA: 51.74 cm (CEP)), (c) mean location error and mean link error.

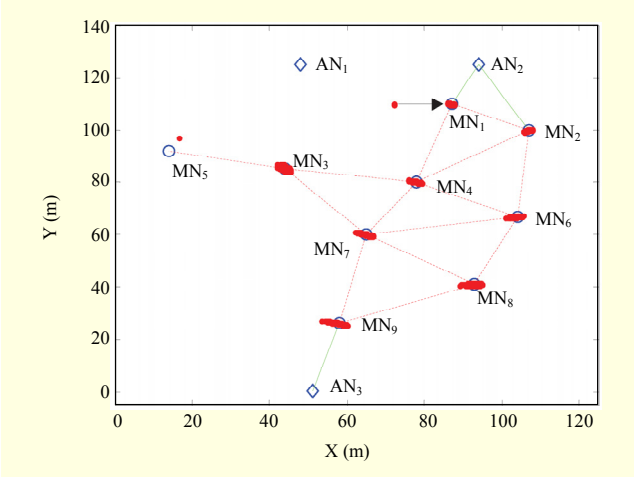

Fig. 8. Simulation results when MN_1 moves and AN_1 and MN_1 are disconnected.

V. Concluding Remarks

An IR-UWB-based cooperative localization method was considered in this paper. Using IR-UWB based on IEEE 802.15.4a, accurate ranging and localization can be achieved. The ranging coverage of the IR-UWB is short, however, owing to the FCC restriction of the transmit power. This factor causes a poor geometric relation among the mobile and anchor nodes. Even worse, the application of IR-UWB cannot be continued owing to this factor. To recover from this problem, a cooperative localization concept was used. Based on this research motivation, in this paper, the CLM-SA was first described. The mobile nodes owned by pedestrians with the same objective can be localized sequentially using this algorithm. However, this method has some structural and implemental problems. To solve this problem, the CLM-BA was proposed. When the mobile nodes cannot be localized based on the CLM-SA owing to the structural problems of the CLM-SA, the location of the mobile nodes can be estimated using the proposed CLM-BA and the management concept of the algorithm. The singular problem that can occur owing to a poor geometric relationship among nodes was solved. Moreover, to localize a mobile node connected to just one reference node, the RAM was presented. The localization performance of the CLM-BA is slightly better than the CLM-SA because of the enhanced geometric relationship between nodes and tips on a successful implementation of the CLM-SA. A thorough evaluation of the performance of the proposed method was carried out by considering several examples of mobile node localization.

It is expected that the proposed method can provide an efficient manner for the localization of a group of pedestrians in special locations, such as soccer fields, amusement parks, and fire or battle locations, where the number of anchor nodes is insufficient for covering the entire application area.

References

[1] K.W. Kolodziej and J. Hjelm, *Local Positioning Systems: LBS Applications and Services*, Taylor & Francis Group, 2006.

[2] H.J. Bang et al. "Location Determination in Wireless OFDM System," *ION GNSS 18th ITM*, Sept. 13-16, 2005, pp. 2213-2217.

[3] J.J. Caffery and G.L. Stuber, "Overview of Radiolocation in CDMA Cellular Systems," *IEEE Commun. Mag.*, vol. 36, no. 4, Apr. 1998, pp. 38-45.

[4] C. Drane, M. Macnaughtan, and C. Scott, "Positioning GSM Telephones," *IEEE Commun.*, vol. 36, no. 4, Apr. 1998, pp. 46-59.

[5] H.S. Ahn and W.P. Yu, "Environmental-Adaptive RSSI-Based Indoor Localization," *IEEE Trans. Autom. Sci. Eng.*, vol. 6, issue 4, Oct. 2009, pp. 626-633.

[6] B. Alzvi and K. Pahlavan, "Modeling of the TOA-Based Distance Measurement Error Using UWB Indoor Radio Measurement," *IEEE Commun. Lett.*, vol. 10, issue 4, Apr. 2006, pp. 275-277.

[7] M. Bocquet, C. Loyez, and A. Benlarbi-Delai, "Using Enhanced-TDOA Measurement for Indoor Positioning," *IEEE Microw. Wireless Components Lett.*, vol. 15, no. 10, Oct. 2005, pp. 612-614.

[8] S.Y. Cho and S.J. Yun, "Efficient Fingerprint DB Generation Method for Indoor Wireless Location Using the Environment Analysis Tool," *ION ITM*, Anaheim, CA, USA, Jan. 2009, pp. 793-797.

[9] F. Forno, G. Malnati, and G. Portelli, "Design and Implementation of a Bluetooth Ad Hoc Network for Indoor Positioning," *IEE Proc.-Softw.*, vol. 152, no. 5, Oct. 2005, pp. 223-228.

[10] B. Li et al., "Method for Yielding a Database of Location Fingerprints in WLAN," *IEE Proc.-Commun.*, vol. 152, no. 5, 2005, pp. 580-586.

[11] S. Saha et al., "Location Determination of a Mobile Device Using IEEE 802.11b Access Point Signals," *IEEE Wireless Commun. Netw. Conf.*, Mar. 16-20, 2003, pp. 1987-1992.

[12] S. Li et al., "Neural Network Based Mobile Phone Localization Using Bluetooth Connectivity," *Neural Comput. Appl.*, vol. 23, no. 3-4, Sept. 2013, pp. 667-675.

[13] J. Albowicz, A. Chen, and L. Zhang, "Recursive Position Estimation in Sensor Networks," *Proc. IEEE Int. Conf. Netw. Protocols*, Nov. 2001, pp. 35-41.

[14] S. Capkun, M. Hamdi, and J.P. Hubaux, "GPS-Free Positioning in Mobile Ad Hoc Networks," *Proc. 34th IEEE Hawaii Int. Conf. Syst. Sci.*, Jan. 2001.

[15] Y.T. Chan and K.C. Ho, "A Simple and Efficient Estimator for Hyperbolic Location," *IEEE Trans. Signal Process.*, vol. 42, no. 8, Aug. 1994, pp. 1905-1915.

[16] X. Ji and H. Zha, "Sensor Positioning in Wireless Ad-hoc Sensor

Networks Using Multidimensional Scaling," *INFOCOM*, 2004, pp. 2652-2661.
[17] Y.S. Nam et al., "Wirelessly Synchronized One-Way Ranging Algorithm with Active Mobile Nodes," *ETRI J.*, vol. 31, no. 4, Aug. 2009, pp. 466-468.
[18] N. Patwari et al., "Relative Location Estimation in Wireless Sensor Networks," *IEEE Trans. Signal Process.*, vol. 51, no. 8, Aug. 2003, pp. 2137-2148.
[19] C. Savarese, J.M. Rabaey, and J. Beutel, "Locationing in Distributed Ad-hoc Wireless Sensor Networks," *Proc. ICASSP*, May 2001, pp. 2037-2040.
[20] A. Savvides, H. Park, and M.B. Srivastava, "The Bits and Flops of the N-hop Multilateration Primitive for Node Localization Problems," *Proc. Int. Workshop Sensor Nets. Appl.*, Sept. 2002, pp. 112-121.
[21] I. Guvenc, Z. Sahinoglu, and P.V. Orlik, "TOA Estimation for IR-UWB Systems with Different Transceiver Types," *IEEE Trans. Microw. Theory Technique*, vol. 54, no. 4, 2006, pp. 1876-1886.
[22] S. Gezici et al., "Localization via Ultra-Wideband Radios," *IEEE Signal Process. Mag.*, vol. 22, issue 4, July 2005, pp. 70-84.
[23] S. Gezici and H.V. Poor, "Position Estimation via Ultra-Wide-Band Signals," *Proc. IEEE*, vol. 97, no. 2, Feb. 2009, pp. 386-403.
[24] S.Y. Cho and Y.W. Choi, "Access Point-less Wireless Location Method based on Peer-to-Peer Ranging of Impulse Radio Ultra-Wideband," *IET-Radar, Sonar Nav.*, vol. 4, issue 5, Oct. 2010, pp. 733-743.
[25] H. Wymeersch, J. Lien, and M.Z. Win, "Cooperative Localization in Wireless Networks," *Proc. IEEE*, vol. 97, no. 2, Feb. 2009, pp. 427-450.
[26] I. Biton, M. Koifman, and I.Y. Bar-Itzhack, "Improved Direct Solution of the Global Positioning System Equation," *J. Guidance, Control, Dynamics*, vol. 21, no. 1, Jan.-Feb. 1998, pp. 45-49.
[27] J.M. Mendel, *Lessons in Estimation Theory for Signal Processing, Communications, and Control*, Prentice-Hall International, 1995.
[28] C.H. Park and K.S. Hong, "Mode-SVD-Based Maximum Likelihood Source Localization Using Subspace Approach," *ETRI J.*, vol. 34, no. 5, Oct. 2012, pp. 684-689.
[29] S.Y. Cho et al., "Innovative Localization System for the Soldier/Fire-Fighter Based on the IR-UWB," *ION GNSS*, Portland, OR, USA, Sept. 21-24, 2010.

Seong Yun Cho received his BS, MS, and PhD degrees from the Department of Control and Instrumentation Engineering at Kwangwoon University, Rep. of Korea, in 1998, 2000, and 2004, respectively. In 2003, he was with the Automation and System Research institute (ASRI), Seoul National University, Rep. of Korea, as a research assistant. In 2004, he was with the School of Mechanical and Aerospace Engineering, Seoul National University, Rep. of Korea, where he was a postdoctoral fellow, BK21. From 2008.09 to 2013.08, he was with ETRI, Rep. of Korea, as a senior member of research staff. From 2008.03 to 2013.02, he was with the Mobile Communication & Digital Broadcasting Engineering Department University of Science & Technology (UST), Rep. of Korea, as an adjunct assistant/associate professor. Since 2013.09, he has been with the Department of Applied Robotics, Kyungil University, Rep. of Korea, as an assistant professor. His research interests include positioning and navigation systems, filtering theory for linear/nonlinear systems, and telematics application systems.

Joo Young Kim received his BS degree in electrical and computer engineering from Information and Communications University (ICU), Rep. of Korea, in 2008, and his MS degree in electrical engineering from the Korea Advanced Institute of Science and Technology (KAIST), Rep. of Korea, in 2010. Since 2010, he has been with ETRI, Rep. of Korea, as a researcher. His research interests include indoor positioning systems, fingerprint-based localization, filtering theory, and augmented reality applications.

Munkhzul Enkhtur received his BS degree in information technology engineering from the School of Information and Telecommunication at Mongolian University of Science and Technology, Mongolia, in 2007. Since 2008, he has been with the Department of Mobile Communication & Digital Broadcasting at the University of Science and Technology, Rep. of Korea, as a PhD candidate in an MS/PhD integrative program. His research interests include navigation technologies and filtering theory.